

Embedded Contact Surfaces in Constitutive Models for Cementitious Composite Materials

T. Bennett[†], A.D. Jefferson[†] & S.C. Hee[†]

[†]*Institute for Theoretical and Computational Mechanics*

University of Cardiff

CF24 0YF

bennettT2@cf.ac.uk

1. INTRODUCTION

This contribution records the development of a general three dimensional constitutive model for cementitious composite materials (CCMs) [1] [2] [3]. This model uses the concept of embedded contact surfaces for the simulation of micro and macro crack opening and closing behaviour, including shear contact.

Validation of numerical models is of paramount importance, to this end, results of benchmark experiments are reported [4]. The subsequent FE analysis of these experiments is then described.

The analysis is far from trivial requiring changes in boundary conditions and material properties in order to create the loading paths produced experimentally. In addition, the control of the experiments with a servo control loop is replicated numerically using local arc-length control [5] [6].

2. NOVEL EXPERIMENTS

In this contribution hexagonally shaped specimens are tested under compression. Upon the attainment of damage in the form of diffuse cracking, seen as non-linearity in the load-deflection graph, the specimen is unloaded and consequently rotated 60⁰ and loaded again until failure. The machine stroke is controlled via a displacement transducer. Two transducers are placed on either side of the specimen, one is positioned vertically and the other is positioned at 60⁰ to the first transducers.

In an attempt to reduce the effect of boundary friction, PTFE sheeting is used between the specimens and the platens.

The transducers are attached to the specimens on small diameter (2.3mm) rods, which are cast into the specimens. The transducer holders are held in place on the rods with screws. The heads of the transducers are captured in small recesses allowing only small rotation of the transducers to occur.

3. NUMERICAL MODEL FRAMEWORK

The framework of the numerical model is described in detail by Jefferson [1],[2], [3], here only a brief overview of the model is given. The essential elements of the model are:

- A local stress - strain relationship, which here is a damage-contact model
- A function from which local strains can be computed such that the local and global constitutive relationships are both satisfied. This is termed the total-local function.
- A triaxial plasticity component for simulating frictional behaviour and strength increase with triaxial confinement
- A thermodynamically consistent global stress-strain relationship The model has been developed with an implicit stress recovery - consistent tangent matrix algorithm, which is described in full by Jefferson [2].

3.1. Local damage-contact relationships. The local stress comprises two components the undamaged component and the damaged contact component, as follows

$$s_i = [H_c D_L e_i] + [H_f(e) \omega_i D_L g_i] \quad (1)$$

where s_i , e_i , D_L are the local stress, local effective strain and local elastic constitutive matrix respectively for damage plane i . s_1 and e_1 denote normal components and s_2 , s_3 and e_2 , e_3 , shear components of the local stress and strain vectors respectively. H_f is a function that varies from 1 to 0 with the increasing crack opening parameter eg, representing the fully debonded material, this simulates the observed phenomena that the wider a crack is open, the less the shear that can be transferred across it. H_c represents the undamaged material and can be expressed as

$$H_c = 1 - \omega_i \quad (2)$$

where, ω_i is a damage variable that lies in the range 0 to 1 and depends upon a local strain parameter ζ_i . g_i is the strain relative to a contact surface. It is related by a transformation to the local strains e_i , as follows;

$$g_i = \Phi_d e_i \quad (3)$$

In the Interlock region $\Phi_d = \Phi_g$ and takes the form

$$\Phi_g = \frac{1}{1 + m_g^2} \left(\left(\frac{\partial \phi_{int}}{\partial e} \right) \cdot \left(\frac{\partial \phi_{int}}{\partial e} \right)^T + \phi_{int} \frac{\partial^2 \phi_{int}}{\partial e^2} \right) \quad (4)$$

where $\phi_{int}(e) = m_g e_1 - \sqrt{e_2^2 + e_3^2}$ and in which m_g is the slope of the Interlock contact surface.

$$s_i = D_L [H_c + H_f \omega_i \Phi_d] e_i = D_L M_{x_i} \quad (5)$$

The effective local strains e_i are those that apply to a fracture process zone of an effective crack plane. They are taken as equal to the relative displacements across the zone divided by the effective zone width w_c . The advantage of using e_i as the basis for the local model is that these local strains (or relative displacements) can be measured directly from tests. However, it is the inelastic component of these strains e_f that is required in the global stress-strain relationship, but it is e , not e_f , that is derived from the total-local function described below and therefore e_f is eliminated from the global stress-strain relationship by the use of equation 6. The inelastic local strain vector is given by

$$e_f = (I - M_x) e \quad (6)$$

The local damage function $\phi(e, \zeta)$ is asymptotic to an equivalent strain friction surface and is orthogonal to normal strain axis at its intercept with that axis, i.e. at $e_1 = \zeta$, $e_2 = e_3 = 0$.

$$\phi(e, \zeta) = \frac{e_1}{2} \left[1 + \left(\frac{\mu_\varepsilon^2}{r_\zeta} \right) \right] + \frac{1}{2r_\varepsilon^2} \sqrt{(r_\varepsilon^2 - \mu_\varepsilon^2 e_r^2 + 4r_\varepsilon^2) (e_2^2 + e_3^2)} - \zeta \quad (7)$$

The material constants r_ε and μ_ε are the relative shear strain intercept and the asymptotic shear friction factor respectively. These are the strain equivalents of the relative shear stress intercept $r_\sigma = c/f_t$ and the asymptotic friction factor μ , noting that c is the shear stress intercept.

3.2. Overall stress-strain relationship. The global stress-strain relationship is given by

$$\sigma = D_e \left((\varepsilon - \varepsilon_p) - \sum_{j=1}^{n_p} N_j^T (I - M_{x_j}) e_j \right) \quad (8)$$

in which D_e is the elastic tensor, σ the stress tensor, ε the strain tensor and ε_p the plastic strain tensor, and n_p = number of damage planes. N_i is the stress transformation matrix such that

$$s_i = N_i \sigma \quad (9)$$

Then applying the transformation equation 9 and using equation 5 and equation 6 the stress recoverable-strain relationship may be obtained to be;

$$\sigma = \left(I + D_e \sum_{j=1}^{n_p} N_j^T (M_x^{-1} - I) C_L N_j \right)^{-1} D_e (\varepsilon - \varepsilon_p) \quad (10)$$

in which $C_L = D_L^{-1}$ and I denotes the identity matrix (tensor).

3.3. Total-Local Function. One of the key components of the model is the Total-Local vector function, and it is use of this function that allows the local and global constitutive relationships, as well as the stress transformation equation 9, to be simultaneously satisfied for multiple damage planes. The model therefore has full coupling between damage surfaces. The function, shown below, gives the error between the transformed global stresses computed from equation 10 and the local stresses computed from equation 5. This is equated to zero and solved for the unknown local strains e_i

$$f_{e_i} = N_i \sigma - s_i \quad (11)$$

When more than one damage plane is present, a nonlinear solution procedure is required for equation 11, but it has been found that very few iterations of a Newton procedure are required to achieve convergence of equation 11 when multiple surfaces are active.

3.4. Plasticity Component. The plasticity component uses a triaxial yield surface developed from the yield function used by Lubliner et al. [8] but it is rounded using the well-known Willam and Warnke [9] function. A similar function form is used for the plastic potential, but a dilatancy parameter is included that controls the slope of the straight meridians. If this parameter is set to unity the potential takes the same form as the yield function and the plastic flow is associated, whereas if is set to zero, the model predicts zero dilatancy. The surface change shape according to a friction hardening/softening function that is dependent upon a plastic work parameter. The tensile apex of the yield surface is not an issue because the damage component of the model ensures the apex is never reached.

4. NUMERICAL RESULTS

The force-displacement response of the numerical analysis is here compared with that determined experimentally 1.

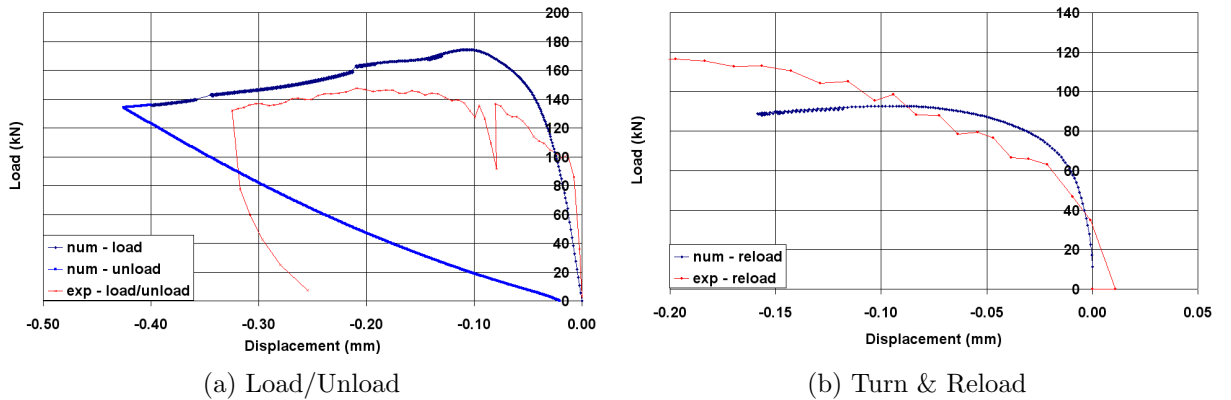


FIGURE 1. Force-Displacement Response

Whilst the general shape of the initial loading agrees with the experimental results, the assumption of the numerical model of secant unloading is seen to be unrealistic (fig1a).

Upon reloading the specimen at 60° to the initial loading angle a limited response was obtained numerically. However, the general shape of the force-displacement response is seen and more pertinently the reduction of the peak load as seen experimentally is also captured.

Contours of the peak strains (fig2a) at the end of the numerical response show significant strains in the areas of damage as induced in the specimen during the initial loading/unloading

cycle of the experiment. Additionally, high strains are encountered where significant damage is observed experimentally (fig2b) in the new loading configuration.

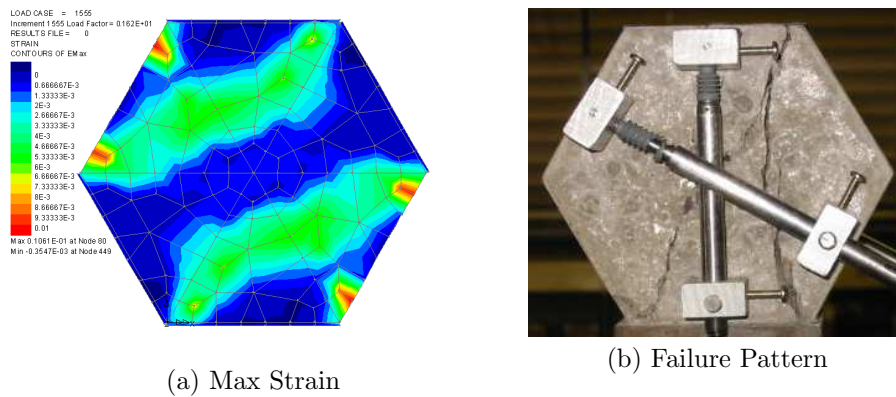


FIGURE 2. Force-Displacement Response

5. CONCLUSIONS

The *CRAFT* constitutive model for cementitious composite materials is outlined including recent developments.

Novel experimental results for the benchmark testing of constitutive models for concrete are presented along with the initial attempts by the authors to replicate the experiments numerically.

Future developments of the constitutive model include the semi-regularisation for strain softening phenomena using Mesmar visco-plasticity and the use of micromechanics as an underlying basis to account for the effects of cracks and inclusions.

REFERENCES

- [1] Jefferson, A.D. Craft - a plastic-damage-contact model for concrete. I. Model theory and thermodynamic considerations, *Int J Solid & Structures*, 40(22), 5973-5999, **2003**
- [2] Jefferson, A.D. Craft - a plastic-damage-contact model for concrete. II. Model implementation with implicit return-mapping algorithm and consistent tangent matrix, *Int J Solid & Structures*, 40(22), 6001-6022, 2003
- [3] Jefferson, A.D. Barr, B.I.G. Bennett, T. and Hee, S.C. Three dimensional finite element simulations of fracture tests using the Craft concrete model, *Computers and Concrete*, 1(3), 261-284, **2004**
- [4] Bennett, T. Jefferson, A.D. and Hee, S.C. Development of an experimental method to determine the effects of cross-cracking in concrete, In preparation, **2005**
- [5] Lusas User manual v13.5, FEA Ltd, **2002**
- [6] Alfano, G. and Crisfield, M.A. Solution strategies for the delamination analysis based on a combination of local-control arc-length and line searches, *Int J Num Meth Engng*, 58, 999-1048, **2003**
- [7] Bennett, T. Askes, H. and Jefferson, A.D. Mesoscopic modelling of concrete under compressive loading, 12th Annual ACME conference Cardiff, Rees, S.R. and Bennett, T. eds, **2003**
- [8] Lubliner, J. Oliver, J. Oller, S. and Onate, E. A plastic-damage model for concrete. *Int. J. Solids & Structures*, 25(3), 299-326, **1989**
- [9] K. Willam, E. Warnke. Constitutive models for triaxial behaviour of concrete. *Proc. Int. Assoc. Bridge Struct. Engng*. Report 19, Zurich, Switzerland, 1-30, **1975**